NTU Journal for Renewable Energy (2022) Vol. 3 (1): 33 -43
DOI: https://doi.org/10.56286/ntujre.v3i1

Influence of Micro-Controller-Based Single Axis Solar Tracker System on Solar Panel's Performance: Case Study

Saman S. Jaafar*, Hiwa Abdlla Maarof

saman.jaafar@uoh.edu.iq, hiwaa2006@gmail.com

Department of Physics, College of Science, University of Halabja, Halabja, KRI, Iraq.
***Corresponding author:** saman.jaafar@uoh.edu.iq
Co-other: Hiwa Abdlla Maarof: Email: hiwaa2006@gmail.com

Received: 30-08-2022, **Accepted:** 12-09-2022, **Published online:** ***15-09-2022

Abstract. There is governmental, academic, and business interest in new emerging renewable energy sources, such as solar energy. In particular, how and how much it produces energy and the environmental impact of these sources. To highly benefit from renewable energies, new methods should be utilized. In this paper, the Microcontroller Arduino Uno board has been used and programmed by Arduino software to build a system as a photo-sensor (Active) Single Axis Solar Tracker System (SASTS). The system was created using a solar panel, two Light Dependent Resistance (LDR) have been used on the two sides (north/south) of the photovoltaic (PV), and a servo motor is connected to the Uno board. The tracking system is constructed to procure the data using the Microcontroller Uno board and specially designed mechanical base. Based on the extracted results, the influence of the SASTS on increasing the solar panel performance is more evident than the outcome Maximum Power Point (MPP) of MATLAB Simulink. Continuously, the SASTS searches for the sun and its position in the sky and puts the PV direct to the sun. Significantly, the tracker system raises the power ratio of the PV. As a result, it significantly increases the solar panel's performance and increases by 55.2% on average during the daytime.

Keywords: *Single Axis Solar Tracker System (SASTS), Arduino Uno board, LDR, Photovoltaics, Servomotor, Solar Panel, MATLAB Simulink.*

Introduction

The more asking for necessary energy supports like electricity, thermal, etc., the Industrial Revolution caused the weather and global warming. On another side, fossil fuels, water, and other energy sources are temporary sources, and they will finish soon. Fossil fuels are the primary source of energy globally. Based on the study of P. K. Devan et al. [1], the fossil fuel-based energy resource has a significant impact on the global warming situation. T. Rajesh et al. [2] claimed that due to natural causes and human activities such as global warming and greenhouse gasses, the climate has reached a critical situation. Akhil Raj K R et al.

[3] claimed that fossil fuel is a supplier of 85% of energy production, and fossil fuel has cost effectiveness and cost changing based on needs and use. Overconsumption of these kinds of nonrenewable energies could contribute to global warming due to the massive emissions. The problems related to fossil fuels and severe environmental concerns have motivated sustainability and green energy efforts. To this end, the researchers have tried to utilize solar as renewable energy to vanish those factors. Solar energy is mainly recommended to solve electrical energy demands, known as renewable energy. C. Pavithra et al. [4] stated that solar energy is

highly recommended as an energy source among all available renewable energy resources due to many benefits, such as continuity of a source without pollution. Solar cells, also called photovoltaic cells, directly convert sunlight into electricity. Photovoltaics is converting light (photons) to electricity (voltage), which is called the photovoltaic effect. Edmond Becquerel explained the essential operation of the solar cell in 1839 [5]. PV is not introducing any pollution (carbon dioxide) to the environment, and solar panels' energy source is the sun, which is an infinite source of energy [5]–[9].

Much research on PV like structure physics, cell combination, solar cell design, and model interfacing problems. However, using PV panels in the long term with the grid power can prevent the distribution of the wires and network and supply the yearly national grid's power cut-offs. It is used for drying mechanisms and significantly boosts the renewable energy supply sources, as is stated in [8]–[10]. There are many reasons to go forward for investment in solar energy, such; as being environmentally friendly, taking Off-the-Grid system, handling the underutilized lands, less loss in the electricity, increasing job opportunities and growing economically, and the, more important that it is a free source and infinite energy. Nevertheless, like in any other field, there are many obstacles to the full benefits of solar energy. One of the main challenging problems is that the sun is continuously Moving in the sky, the irradiance angle on the PV's surface will change continuously, resulting in the produced energy being directly changed. Changing with the radiation's intensity due to the irradiance's deflection angle; Obviously, the PV's power energy depends on arrived light energy. The average angle radiation of the sunlight on the PV is highly absorbed, which means the light energy at 90 degrees shines on the solar panel. Due to the continuous change of the sun's position, the sun's energy does not completely arrive on the solar panels during the daytime. Consequently, the Solar Tracker System (STS) has become a crucial issue for harvesting energy from the sun during the daytime and solving that problem [6], [11], [12]. The solar tracking system can be deployed automatically on Earth A. Barbónet al. [13]. Sensors are used to detect the position of the sun and the controller controls the motor rotation to move the solar module such that it is facing the sun most of the time Md. T. A. Khan et al. [14]. The tracker systems continuously search and find the sun's exact position and the output of electric energy will be increased [11]. O. C. Ozerdem and A. Shahin [15] noted that the maximum efficiency of the PV depends on the normal irradiance of the radiation on its surface. The tracking photovoltaic system can be divided into photo sensor-based (LDR) STS and time-based STS. Both types can be divided into a single-axis tracking system and a dual-axis tracking system [6], [7], [16], [17]. The efficiency of the (PV) depends on the two significant factors, such as irradiance angle and the time of irradiance on the surface of the PV [11], [15], [17], [18]. Therefore, the solar radiation angle is better to be standard on the solar panels for harvesting the maximum possible power. Consequently, the best STS are central to the performance of the PV system. M. A. Vaziri Rad et al. [19] showed that using STS caused to decrease in the number of panels and cost. S. Sumathi et al. [20] practically achieved the STS's efficiency of PV by the dual-axis tracker system with having feedback control, four LDRs as an optical sensor with simple electronics circuit. The STS can use as a water heating process which is tested for two types of the outlet solar. The dual tracking technology raised the water temperature significantly [10], [21]. M. Das and E. K. Akpinar [22] noted that the STS also could be used in the dryer process. M. A. Vaziri Rad et al. [19] reported that vertical STS is cost-efficient and increases the efficiency of the solar grid by 23% on average. M. Ghassoul [23] demonstrated that the various achieved energies from the fixed PV and dual-axis PV are differed by 12% and 69%, respectively, while C. Jamroen et al. [24] reported that the difference is about 44.89%t for such a similar case. Based on the study of T. Hong et al. [7] The indirect 2-axis hybrid solar tracking system can be established in different geographic contexts by changing the geographical parameters used to calculate the hourly altitude and azimuth of the sun. On the other hand, H. Zlatanov and G. Weinrebe's [25] presented a new method to create a database of heliostats, Concentrate Photovoltaics CPV, and PV trackers that allow end-users to choose an economic system for their site under considering the local environmental conditions and country codes. The hybrid solar tracker proposed by J. K. Tharamuttam and A. K. Ng [26] could harness the optimal solar energy in all weather conditions with a large-scale implementation, considerably reducing carbon emissions and cutting electricity costs for public and private organizations. M. Mirdanies's [27] showed that by using the algorithm, the tracker could work in two angles of freedom which makes it more accurate. Fuzzy logic has been executed by A. Zakariah et al. [12] to guarantee finding the maximum point of the power quickly. An LDR sensor was used to detect solar irradiance and the sun's positional change. The sensor continuously monitors the solar radiation, and then the data are transferred to the power window motor via the Arduino UNO microcontroller. N. Raju [28] concluded that the most widely used solar tracking control strategy is the closed loop, representing 54.39% of all the publications consulted. On-off, fuzzy logic, proportional-integral-derivative, and proportionalintegral control algorithms are most applied in active solar tracking systems, representing 57.02%, 10.53%, 6.14%, and 4.39%, respectively, as reported by

R. F. Fuentes-Morales et al. [29]. Based on Aldair et al. [30] research outcomes Both dualaxis and single-axis solar tracker system boosted the output power of solar panel by 50.6% and 39.4% compared to the stationary solar panel.

In the current paper, the influence of using a microcontroller-based single-axis photosensor of an automatic solar tracker system has been investigated compared to the fixed angle of the solar panel compared to the ideal case from the MATLAB simulation testing. A small prototype of the solar tracking system using a closed-loop strategy and perturb and observer algorithm was constructed. Light-dependent resistors are used as the sensors of the solar tracker, and a servo motor has been utilized for the rotation of the panel from the west to the east. The microcontroller Uno board is used as the processer of the tracker. The designed tracker has a precise control mechanism that accurately tracks the sun's position in the sky, and the achieved data with their plots are compared to the MATLAB simulation-based test of SASTS. All the experiments and collected data were done in Halabja city in the Kurdistan region/Iraq within two days.

All the planets rotate around the sun and themselves in the solar system. This kind of motion is pretending that the sun is moving, and it is not stationary at a point in the sky. The main goal of the SASTS is to make the solar panel feels like the sun is at a fixed point in the sky. To this end, a systematic device is needed by collecting several parts that integrate and work together to fix the sun's motion in the sky virtually. In this section, the necessary theory regarding the created system is explained with its parts in detail. The detail of the components is shown the various principles of their working in components and a system.

$$\alpha = \sin^{-1}(\cos\varphi \times \cos\delta \times \cos\omega + \sin\varphi \times \sin\delta) \quad (2)$$

While the second angle is given by

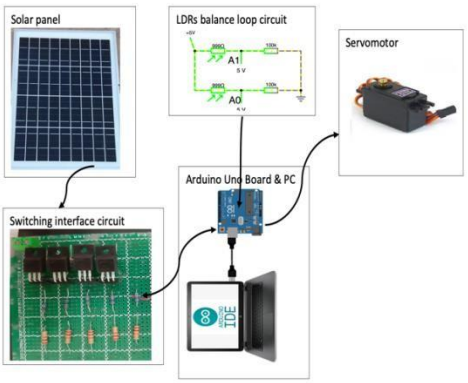

Figure 1: Block diagram of proposed single-axis solar tracker system

Principle of Developed SASTS Systems

Theory of Solar Radiation

The main factor in producing the electricity from the PV is solar radiation. There will be two different beams from the incoming radiation, the first is the perpendicular beam that is mainly absorbed by the PV surface, and the second goes back from the surface of PV, which is reflected from the PV surface. It is an incorrect sentence that the irradiance does not make sense for PV to produce electricity [31]. Equation 1 gives the direct irradiance received on the PV surface, as shown in Figure 1. Equations 1 to 3 have been used from the reference [32].

$$I_D = I_{DN} \cos\alpha \quad (1)$$

where I_D is direct irradiance, α is irradiance angle, and I_{DN} is normal direct irradiance.

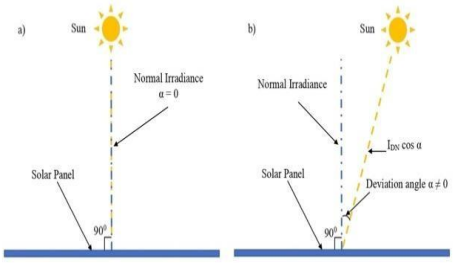

Figure 2: Normal and Non-normal Angle of Irradiance on PV

T_C = Solar Panel's Temperature, °C

T_{C0} = Solar Panel's Reference Temperature, °C

Two angles can determine sun position for the target city (Halabja city): Altitude angle (α) and Azimuth angle (γ) (see Figure 3). These Two angles are given by equation 2 and equation 3, respectively.

$$Cos\gamma \frac{\sin\alpha \; x \; \sin\varphi \; x \; \sin\delta}{\cos\alpha \; x \; \sin\varphi} \quad (3)$$

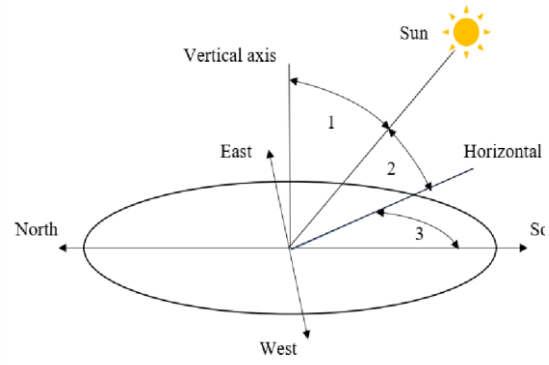

Figure 3: Sun Radiation Angeles Simulation 1: Zenith angle 2: Altitude Angle (α = 35⁰) 3: Azimuth Angle

Altitude and azimuth angles of Halabja city depend on local altitude (α = 350), solar declination angle (δ = 50), and hour angle (ω), and they estimate as proved in equation 3 [32], [33].

Obviously, In Figure 3, it can be sensed that the irradiance is decreasing over time due to the sun's motion in the sky and changing the angle of irradiance.

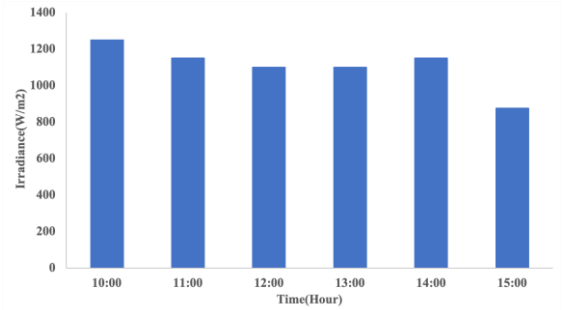

Figure 4: Variation of Irradiance with Time

Temperature effectiveness on Photovoltaic

Clearly, the temperature of PV has specific effectiveness on the performance of the solar panel as equation 4 [34] and it can be seen more understandable from Figure 5.

$$I_L(T_c - T_{c0}) = \frac{\Phi}{\Phi_0}[I_{L0} + K_{I,SC}(T_c - T_{c0})] \quad (4)$$

where I_L = Solar Panel's Current of Irradiance based on Changing on Temperature, A

I_{L0} = Solar panel's Current at Reference Condition, A

= Irradiance, W/m^2

$_0$ = Reference Irradiance, 1000W/m^2

$K_{I,SC}$ = Temperature Coefficient of the Short Circuit Current, A/°C

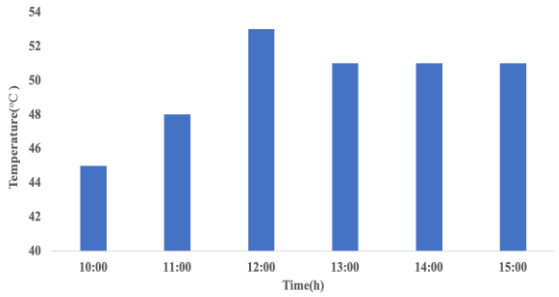

Figure 5: Change in Temperature with Time

SASTS Parts

Mechanical Base structure

Aluminum makes the mechanical base of SASTS, and it is lightweight and connected to a servo motor. The overall dimension of the structure is 30 cm, 25 cm, and 25 cm. The base structure has a holder, gear shaft, panel holder, and servo motor holder, as shown in Figure 5. Furthermore, the geometry of the base structure also affects the cost [25].

Arduino board

Main advantages are fast processing and easy interface. These open-source boards provide free or virtually low costs, highly reliable, and affordable technology [35]. The analog pins (A0A1) received the signal from the different parts of SASTS. For example, A0 and A1 are getting signals from the LDRs. A2, A3, A4, and A5 get the various outcome voltages from the switching circuit. Also, the Uno board could be connected through USB type B to the computer and upload the proper code through Arduino Integrated Development Environment (IDE). The Uno board could be working by loading a voltage between 9-20V, but all I/O pins only support 5V voltage [36].

LDRs

The commonly used semiconductors are cadmium Sulphide, lead Sulphide, germanium, silicon, and gallium arsenide [37]. LDR is an abbreviation of Light Dependent Resistor; it is a semiconductor. The resistance of LDR depends on changing of light's intensity; they change inversely [31].

Servomotor

A rotary or linear actuator allows for precise control of angular or linear position, velocity, and acceleration. The High-Torque Metal Gear

Servo Motor for Robotics (MG996R) Digital Servo, which
is used in the current study, can be rotated approximately 1 20 degrees, lifting about 10Kg weights [6], [38], [39].

1. Lower heating of the motor for the same torque due to a smaller number of turns per coil.
2. A minor moment of inertia and smaller total mass.
3. Lower manufacturing cost.

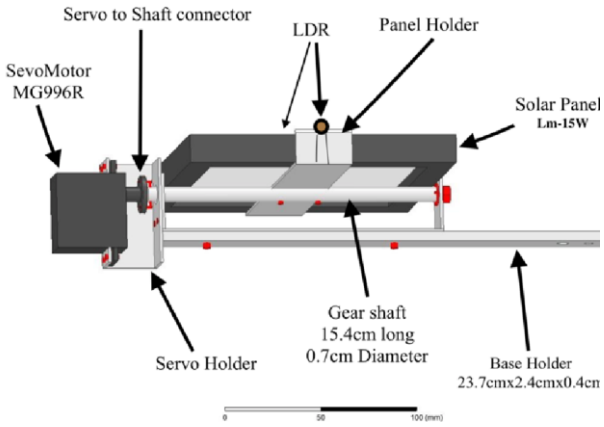

panel is fixed.

Figure 6: Mechanical Structure of SASTS [40]

Solar panel

The used solar panel can be considered as a lightweight and its specifications are listed in Table 1.

Table 1. *Specification of LM-15W Solar Panel Model*

Parameters	Curren (A)	Voltage(V	Power(W)
Maximum Power	--	--	15
Open Circuit Voltage	--	21.6	--
Short Circuit Current	0.89	--	--
Peak Power Voltage	--	18	--
Peak Power Current	0.83	--	--

Switching Interface Circuit (SIC)- Electronic Control Units for SASTS

From Equation 5 and 6, if $R_1 = R_2 = 22K\Omega$, $V_{LDR1} = V_{LDR2} = V_s = 5V$, and then $R_{LDR1} = R_{LDR2}$.

Based on the operation of SASTS, the resistances of both East-LDR and West-LDR depend on the amount of irradiance on both LDRs. Furthermore, A0 and A1 will change based on that irradiance value. Those make the amount of error. From Figure 6, when they have the same irradiance, A0 and A1 have the same value again, location in the sky by LDRs sensors because of the effectiveness of average radiation on the solar panel, which was and the error will be zero, which means the solar

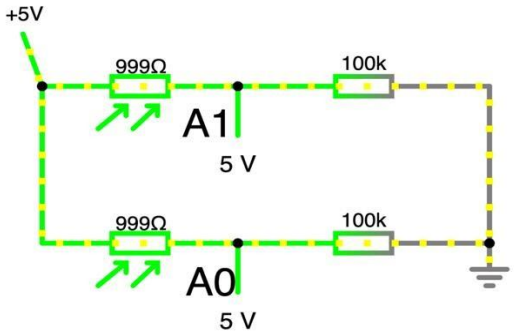

Figure 7: LDRs' Balance Loop Circuit When both LDRs' have Same Brightness

( ) *(5)*

( ) *(6)*

LDRs can be considered the eyes of the system because all the steps depend on the LDRs' sensing. The aim was to find the sun's absorbed mainly by PV based on equation 1. The LDRs lay on both sides of the PV, as shown in Figure 10. The incoming signal from LDRs transfers to the Uno board, and the board will find the amount of difference between A0 and A1. If the difference or error is more than the specified value in the Arduino code, it will send a signal to the servo motor to rotate toward the highlighted LDR. Then the microcontroller passed to the next step, measuring the voltage data and calculating the current and power data from them based on ohm's law. Lastly, P-V curve characterization has been plotted from measurement data. Therefore, the process was as precise in the shown flow chart in Figure 9.

As shown in Figure 7, the SIC is established in some aims, while the solar panel produced a voltage near 21.6V. Meanwhile, those kinds of voltage are harmful and more to read by the Uno board. Previously, digital and analog pins could accept an of 5Vto regular operation. As a result, the SIC board has voltage regulations which consist of resistors R5 to R12 as shown as voltage regulator resistors with a specific value (100KΩ and 22KΩ). Finally, the regulated voltage could be measured by the digital pins of the Uno microcontroller. The goal of putting resistors R1, R2, R3, and R4 is just to protect MOSFETs.

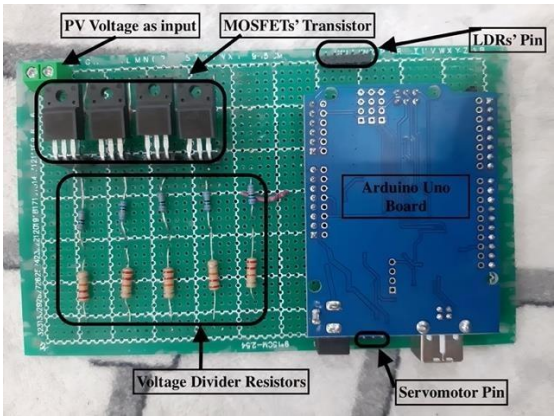

Figure 8: Switching Interface Circuit

The additional aim of SIC is to achieve different measured data of current voltage. Continuously, the MOSFETs' are switching on/off based on the sending signals from digital pins of the microcontroller board. For each step of switching the MOSFETs,' specific power-voltage data can be measured. All regulated voltage process has been done based on Kirchhoff's Voltage Law (KVL), and the proper equation has been written below. The PV voltage (Vpv) and then the voltage on R5 and R10 are calculated using equation 7.

$V_{pv} = V_{R5} + VR_{10}$ (7)

The resistors (R5 and R10) are in series connection; thus, based on Kirchhoff's Current Law (KCL), the current passing through each resistor is equal, so equation 7 can be rearranged as shown in equation 8.

$V_{pv} = IR_5 + IR_{10}$ *and* $P = I*V_{pv}$ (8)

The outcome voltage is determined from the ratio of resistors as equation 9.

$$V0 = \frac{R10}{R5+R10} * Vpv = Vpv = \frac{22}{22+80} * 21.6 = 4.66V \quad (9)$$

When the output voltage of PV is 21.6V and R5=100KΩ and R10=22KΩ, this voltage (4.66V) is acceptable to be read by a micro-controller because it is less than 5V. The (P & O) algorithm of testing SASTS by the simulation-based test, which acts as a virtual lab for measuring the same data to have the best validation. To follow our objective, a simple MPP Simulink circuit has been designed to have ideal power data to compare to an exact testing situation of the SASTS. The benefit of using this way is to verify the achieved power by using the SASTS system compared to MATLAB simulation. Figure 8 is shown the applied circuit in MATLAB Simulink for measuring the ideal data for a similar case of SASTS and fixed solar panel. For that reason, the exact value of irradiance and temperature of a natural experiment of SASTS has been input to the simulation and run when irradiance = 1100 w/m2 and temperature = 50 ^{0}C on average we suppose this value was constant during the time of experimenting.

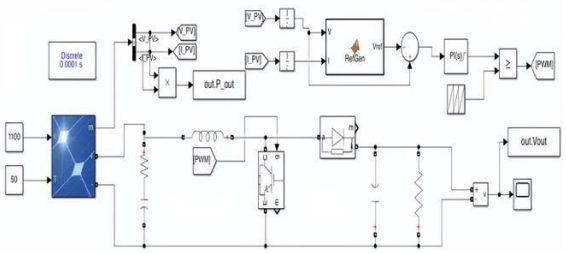

Figure 9: MATLAB Simulation Circuit of PV Characterization

Algorithm for SASTS System

The uploaded code in the Arduino Uno board goes through several steps like the below (P & O) flow chart, shown in Figure 9. Mainly, the tracker system operation depends on the LDRs' resistance value. When the difference in resistance of LDRs shows us the amount of error. Mainly, the error was produced by a difference in light intensity on each LDRs, which caused different resistance values.

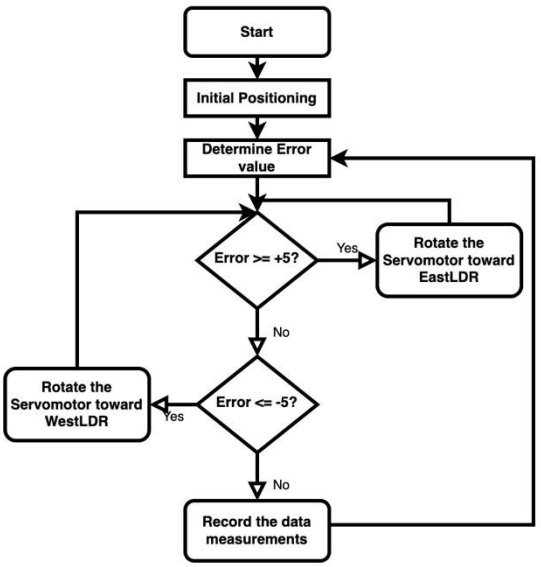

Figure 10: SASTS Working Algorithm

The first step of the code is to check the amount of error among the east-LDR and west-LDR shining by different light intensity the error produced, and the microcontroller sensed that. The second step is for the Uno board to send a signal to the servo motor to rotate in the direction of high shined LDR, and it regularly checks the amount of error. If its value is less than 5 lux (0.04 w/m2), the servo motor stops the rotation. Otherwise, the process continued until the condition had been proved.

However, under proven conditions (|error| < 5), the SASTS would receive the voltage-power measurements data as shown in a part of the experimental result and discussion.

Experimental Results and Discussion

The SASTS system is constructed from Uno board, LDRs, servo motor, SIC, and a solar cell as shown in Figure 11.

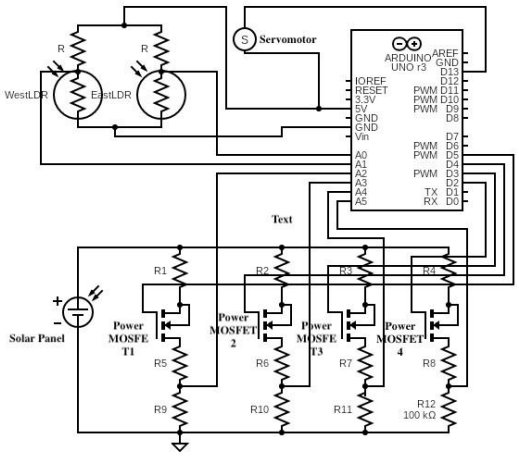

Figure 11: Complete circuit diagram of SASTS

The system weighs about 1 Kg and can be put on the roof, ground, and wall, and two screws could fasten it. The switching circuit board and the microcontroller can join the mechanical base. In Figure 10 the compacted of the system can be seen.

The built system was used for four days in April 2022, from 10:00 a.m. to 3:00 p.m., in Halabja city in the Kurdistan region/Iraq. On each day, the SASTS was operating in both fixed and SASTS ways for each hour, and already the temperature and amount of irradiance were measured for that hour, and the data were taken hourly. In another case, the MATLAB Simulation was used to measure and plot solar panels' ideal power curve characterization. These two different situations aim to prove and show the effectiveness of the SASTS in increasing the power ratio of the PV.

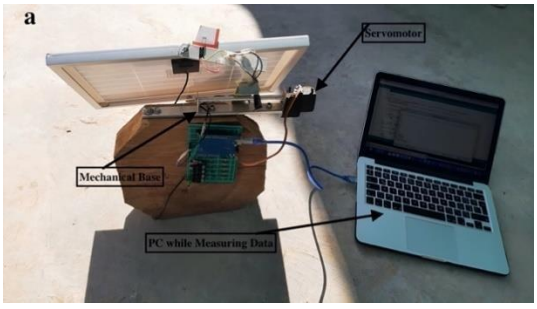

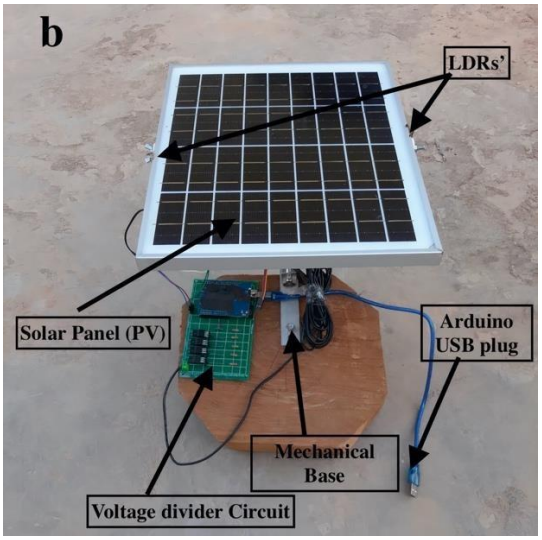

Figure 12: The Over All combined Tracker System, (a) Back of Panel (b) Front of Panel

Figure 11 shows the solar panel characterization Power-Voltage (V-P) curves for SASTS measurements data for six hours and the MATLAB Simulink measurement data. Figure 12 shows the data measurements of solar panel characterization in fixed situations in the same hours. For these cases, the P-V curves characterization has been studied just to find the MPPs and compare them together. Whatever from these MPPs, we can again determine the power ratio for the worth case. Figure 13 shows the differences between Figure 11 and Figure 12, which can be sensed more.

Table 2: Power per Hour data measurements for singleaxis solar tracker system

Power/ W Time: 10:00	Power/ W Time: 11:00	Power/ W Time: 12:00	Power/ W Time: 13:00	Power/ W Time: 14:00	Power/ W Time: 15:00
0.67	0.65	0.67	0.68	0.73	0.52
3.96	3.85	3.96	4.02	4.35	3.07
6.46	6.28	6.44	6.56	7.11	5.02
12.46	12.15	12.42	12.64	13.70	9.64
16.52	16.10	16.43	16.76	18.17	12.57
18.74	18.27	18.64	18.97	20.61	14.18
24.60	24.05	24.48	24.97	27.06	18.61

28.01	27.45	27.94	28.44	30.45	21.18
35.31	34.78	35.58	36.03	38.51	26.80
39.11	38.42	39.30	39.90	42.44	29.58
44.17	43.35	44.40	45.08	48.19	33.65
51.11	50.07	51.25	52.04	55.80	38.98
60.96	59.40	60.96	62.23	66.27	47.21
65.74	63.88	65.57	67.11	71.65	51.00
70.92	68.73	70.37	72.21	76.73	53.42
75.71	73.37	75.32	77.10	82.14	55.63
80.51	78.01	80.09	82.20	87.14	57.85
83.39	81.23	83.61	85.37	90.74	58.37
89.42	86.86	88.95	91.07	96.59	61.94
93.24	90.32	92.26	92.99	97.95	59.91
96.39	90.59	91.34	91.09	93.85	61.20
92.22	88.70	89.95	88.46	91.21	58.53
90.49	84.98	86.96	84.48	84.98	56.13
85.65	82.19	83.91	80.73	81.21	53.07
83.38	78.23	78.71	73.71	72.77	50.96
77.50	72.24	70.37	66.04	64.47	44.01
68.82	63.83	63.83	57.95	53.38	36.45
61.84	57.29	57.72	49.50	45.06	34.29
55.00	52.93	54.17	45.04	41.88	34.57
51.21	48.21	49.40	40.12	35.08	30.39
45.69	43.97	45.11	34.71	30.17	22.59
41.49	37.71	38.42	27.60	24.39	17.00
34.80	32.30	31.97	22.82	17.89	14.54
28.92	26.34	26.94	17.58	12.75	11.54
24.00	22.33	23.16	15.43	9.98	9.53
21.39	19.80	19.93	12.49	0.00	0.00
18.22	17.60	17.60	10.74	0.00	0.00
16.21	15.63	16.21	9.84	0.00	0.00
14.56	13.14	14.01	9.42	0.00	0.00
12.56	12.25	12.45	9.01	0.00	0.00
10.58	11.46	11.36	0.00	0.00	0.00
9.87	9.96	9.96	0.00	0.00	0.00

14.80	12.75	6.40	1.49	0.17	0.15
19.47	16.78	8.39	1.92	0.22	0.19
22.23	19.15	9.54	2.17	0.25	0.21
26.66	24.15	11.96	2.72	0.32	0.26
30.98	26.65	13.23	3.00	0.35	0.28
34.84	30.12	14.80	3.40	0.40	0.32
40.13	34.65	16.89	3.87	0.43	0.00
47.35	40.67	19.74	4.56	0.00	0.00
50.85	43.92	21.16	4.91	0.00	0.00
54.54	46.93	22.41	5.20	0.00	0.00
58.18	50.20	23.94	5.47	0.00	0.00
62.01	53.49	25.24	5.79	0.00	0.00
64.54	55.66	26.10	5.99	0.00	0.00
69.36	60.00	28.01	6.33	0.00	0.00
72.71	62.89	29.08	6.57	0.00	0.00
74.28	64.30	30.56	6.87	0.00	0.00
72.84	63.27	30.99	6.96	0.00	0.00
70.37	60.42	30.83	7.09	0.00	0.00
68.61	58.72	30.30	7.14	0.00	0.00
63.97	54.93	28.34	6.94	0.00	0.00
57.15	49.68	26.43	6.19	0.00	0.00
51.16	44.79	23.41	0.00	0.00	0.00
45.62	40.29	20.83	0.00	0.00	0.00
41.70	38.14	19.48	0.00	0.00	0.00
37.82	33.92	17.59	0.00	0.00	0.00
33.22	30.17	15.88	0.00	0.00	0.00
28.20	24.67	13.32	0.00	0.00	0.00
23.51	19.64	11.14	0.00	0.00	0.00
19.19	15.81	8.87	0.00	0.00	0.00
16.47	13.77	0.00	0.00	0.00	0.00
13.75	11.09	0.00	0.00	0.00	0.00
12.43	9.45	0.00	0.00	0.00	0.00
11.26	0.00	0.00	0.00	0.00	0.00
9.70	0.00	0.00	0.00	0.00	0.00
8.58	0.00	0.00	0.00	0.00	0.00
7.51	0.00	0.00	0.00	0.00	0.00
5.87	0.00	0.00	0.00	0.00	0.00

Simulation

Figure 14: Power-Voltage Curve (MPPs') for Both SASTS &

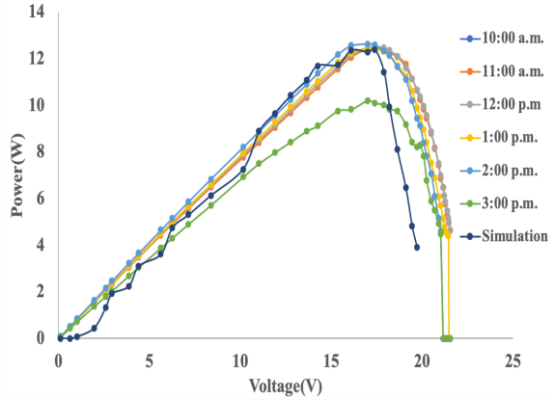

Figure 13: Current-Voltage Curve for Both SASTS &

Simulation

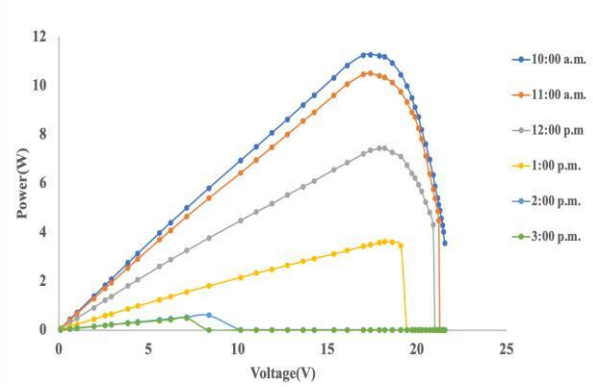

Table 3: Power per Hour data measurements for stationary solar panel

Power/W Time: 10:00	Power/W Time: 11:00	Power/W Time: 12:00	Power/W Time: 13:00	Power/W Time: 14:00	Power/W Time: 15:00
0.53	0.46	0.23	0.06	0.01	0.01
3.13	2.69	1.38	0.33	0.04	0.03
5.10	4.39	2.24	0.53	0.06	0.05

Table 4: Power-Time Measurement Data

MPPs/W		Time/h
Stationary Case	Movable Case	
11.26	12.801	10:00
10.5	12.631	11:00

9.83	8.47	4.29	1.01	0.11	0.10
13.04	11.23	5.67	1.32	0.15	0.13

7.43	12.5106	12:00
3.6	12.444	13:00

0.6	12.4236	14:00
0.48	10.2	15:00

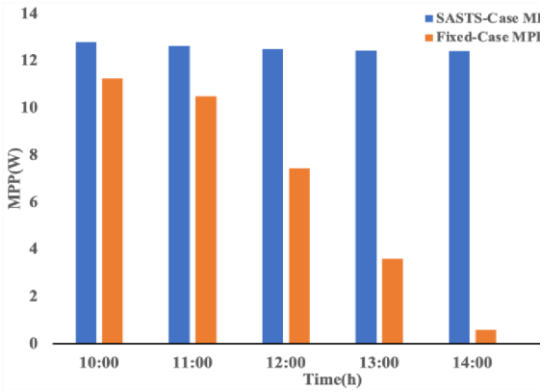

Figure 15: MPPs' for each Hour in both SASTS & Fixed Case

Calculation of the Efficiency

Relative Error of MPPs'

In this part, the effectiveness of the SASTS can be sensed and understood. The boost in solar panel performance is determined by the achieved MPPs while using SASTS, and so more obtained MPP points from Figure 13. The SASTS power points and Simulink power points and the relative error of power can be determined using equation 10.

$$\eta = \frac{SASTS\ Power - Simulation\ Power}{SASTS\ \boldsymbol{Power}} x\ 100 \quad (10)$$

where η is relative error of power of real testing of SASTS and Simulink-based testing of it.

There are two parts of power ratio error:

First between SASTS and MATLAB Simulink

$\eta = \frac{12.63-12.38}{12.63}$ * 100 = 1.98% , this value shows us our experiment result is acceptable and much close to Simulink validation.

and Second between the SASTS and Fixed case as equation 11

$$\eta = \frac{SASTS\ Power - Fixed\ Case\ Power}{SASTS\ \boldsymbol{Power}} x\ 100 \quad (11)$$

$\eta = \frac{10.5-0.48}{10.5}$ * 100 =95.4 % for 10:00 a.m. O'clock and for others we can see in Figure 16.

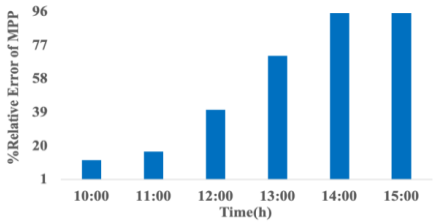

Figure 16: Change of Relatives Error in Power with Time

According to the previous studies, the experimental results and the simulation data by S. S. Jaafar et al. [40], W. Batayneh et al. [41] and B. A. Hamad et al. [42] showed an 11–21% improvement in the tracking system vs. stationary case. The system built by A. Zakariah et al. [12] improved output power efficiency by 18.13% compared to the stationary panel system. Now we can determine the relative error in power for both cases of using SASTS and fixed solar panels in accurate testing and Simulinkbased testing, as shown in Figure 14.

After completing the experiments and analyzing the results, this study showed that the efficiency of the used PV has been heightened by 55.2% and verified by MATLAB Simulation-based MPP. The difference amount depends on the several factors such as the quality of construction of the panel, change of irradiance during the process, power loss due to electronic components in the switching circuit, temperature, pollution, and hourly change in altitude angle, which is caused to have a slight deviation angle toward north and south.

Comparison

This section will give us a brief and much clarification about the influences of the SASTS compared to the MATLAB Simulink and fixed case.

Whatever, from the sketched plots in Figure 15 and Figure 16. In both cases, the MPPs were found. Based on equation 1, the highest luminous intensity is the 0 angles of deviation (normal irradiance) of the sun's rays (1100 w/m^2) and solar panel Temperature 50 ^{0}C. Meanwhile, by using SASTS, the plotted data of mentioned figures have shown that the high amount of the incident rays had been absorbed and changed to electrical energy because the MPP points are high. So more from the fixed solar panel case and high deflection angle, the MPP was less than SASTS cases. The sensible point is that the SASTS system help to remain the solar panel facing the sun and using the regular coming rays. The achieved MPP from SASTS is 55.2% on average when more significant than the MPP of the fixed solar panel case. We can say the SASTS is worked closed to the MATLAB Simulink-based case based on equation 10 and equation 11. Thus, the solar tracker (photo-sensor tracker) effectively boosts the output energy for the PV system.

Conclusion

An automatic solar tracker system that works based on the light sensor optimized the MPP of the solar panel. Combining the LDRs' and servomotor with a microcontroller Uno board made an automatic solar tracker system. Using the automatic or light sensor SASTS aims to achieve the best current and voltage data from the solar panel while sunny daylighting. The accuracy of this tracker system is 0.85 w/m^2. The SASTS increased the MPP of the solar panel verified compared to the Simulink-based test with a small error ratio (%Relative Error MPP = 1.98%) and a significant ratio of improving MPP regarding the fixed solar panel (55.2%). Using the servomotor was a factor in preventing more energy waste because of its advantages. SASTS is a self-supporter energy system because it can supply a low amount of electrical voltage for working all system parts.

Contribution

Saman Jaafar carried out system building, data analysis, and interpretation experiments. Hiwa Abdlla Maarof cooperated as a partner in data analysis. Both authors have read and agreed to the published version of the manuscript.

Declarations

Ethical approval and consent to participate: Not applicable.

Consent for publication: Not applicable.

Conflicts of interest: The authors declare no conflict of interest

References

[1] P. K. Devan, C. Bibin, S. Gowtham, G. Hariharan, and R. Hariharan, "A comprehensive review on solar cooker with sun tracking system," *Mater. Today Proc.*, vol. 33, pp. 771–777, 2020, doi: 10.1016/j.matpr.2020.06.124.

[2] T. Rajesh, K. S. Tamilselvan, A. Vijayalakshmi, Ch. Narendra Kumar, and K. Anitha Reddy, "Design and implementation of an automatic solar tracking system for a monocrystalline silicon material panel using MPPT algorithm," *Mater. Today Proc.*, Oct. 2020, doi: 10.1016/j.matpr.2020.08.635.

[3] R. K. R. Sreejith, S. Amal, R. K. A. Vidhu, and N. K. B. Sanju, "Implementation of an Automatic Solar Tracking System," no. May, pp. 273–276, 2019.

[4] C. Pavithra *et al.*, "A brief overview of maximum power point tracking algorithm for solar PV system,"
Mater. Today Proc., Feb. 2021, doi: 10.1016/j.matpr.2021.01.220.

[5] A. Goetzberger, "Workshop on " Physics for Renewable Energy " Crystalline Silicon Solar Cells," *Int. At. Energy Agency*, pp. 17–29, 2005.

[6] F. M. Hoffmann, R. F. Molz, J. V. Kothe, E. O. B. Nara, and L. P. C. Tedesco, "Monthly profile analysis based on a two-axis solar tracker proposal for photovoltaic panels," *Renew. Energy*, vol. 115, pp. 750–759, Jan. 2018, doi: 10.1016/j.renene.2017.08.079.

[7] T. Hong *et al.*, "A Preliminary Study on the 2-axis Hybrid Solar Tracking Method for the Smart Photovoltaic Blind," *Energy Procedia*, vol. 88, pp. 484–490, Jun. 2016, doi: 10.1016/j.egypro.2016.06.067. [8] O. Ellabban and A. Alassi, "Integrated Economic Adoption Model for residential grid-connected photovoltaic systems: An Australian case study," *Energy Rep.*, vol. 5, pp. 310–326, Nov. 2019, doi: 10.1016/j.egyr.2019.02.004.

[9] J. Zhang, Z. Yin, and P. Jin, "Error analysis and auto correction of hybrid solar tracking system using photo sensors and orientation algorithm," *Energy*, vol. 182, pp. 585–593, Sep. 2019, doi: 10.1016/j.energy.2019.06.032.

[10] R. ElGamal, S. Kishk, S. Al-Rejaie, and G. ElMasry, "Incorporation of a solar tracking system for enhancing the performance of solar air heaters in drying apple slices," *Renew. Energy*, vol. 167, pp. 676–684, Apr. 2021, doi: 10.1016/j.renene.2020.11.137.

[11] N. AL-Rousan, N. A. M. Isa, and M. K. M. Desa, "Advances in solar photovoltaic tracking systems: A review," *Renew. Sustain. Energy Rev.*, vol. 82, pp. 2548–2569, Feb. 2018, doi: 10.1016/j.rser.2017.09.077.

[12] A. Zakariah, M. Faramarzi, J. J. Jamian, and M. A. M. Yunus, "Medium size dual-axis solar tracking system

with sunlight intensity comparison method and fuzzy logic implementation," *J. Teknol.*, vol. 77, no. 17, pp. 145–157, 2015, doi: 10.11113/jt.v77.6468.

[13] A. Barbón, J. A. Fernández-Rubiera, L. MartínezValledor, A. Pérez-Fernández, and L. Bayón, "Design and construction of a solar tracking system for small-scale linear Fresnel reflector with three movements," *Appl. Energy*, vol. 285, p. 116477, Mar. 2021, doi: 10.1016/j.apenergy.2021.116477.

[14] M. T. A. Khan, S. M. S. Tanzil, R. Rahman, and S. M. S. Alam, "Design and construction of an automatic solar tracking system," *Electr. Comput. Eng. ICECE 2010 Int. Conf. On*, no. December, pp. 326–329, 2010.

[15] O. C. Ozerdem and A. Shahin, "a Pv Solar Tracking System Controlled By Arduino / Matlab / Simulink," *Int. J. "Technical Phys. Probl. Eng.*, no. December, pp. 5–10, 2014.

[16] L. M. Fernández-Ahumada, F. J. Casares, J. Ramírez-Faz, and R. López-Luque, "Mathematical study of the movement of solar tracking systems based on rational models," *Sol. Energy*, vol. 150, pp. 20–29, Jul. 2017, doi: 10.1016/j.solener.2017.04.006.

[17] J. Song, Y. Zhu, D. Xia, and Y. Yang, "A Photovoltaic Solar Tracking System with Bidirectional Sliding Axle for Building Integration," *Energy Procedia*, vol. 61, pp. 1638– 1641, 2014, doi: 10.1016/j.egypro.2014.12.315.

[18] M. Abdollahpour, M. R. Golzarian, A. Rohani, and H. Abootorabi Zarchi, "Development of a machine vision dual-axis solar tracking system," *Sol. Energy*, vol. 169, pp. 136–143, Jul. 2018, doi: 10.1016/j.solener.2018.03.059.

[19] M. A. Vaziri Rad, A. Toopshekan, P. Rahdan, A. Kasaeian, and O. Mahian, "A comprehensive study of techno-economic and environmental features of different solar tracking systems for residential photovoltaic installations," *Renew. Sustain. Energy Rev.*, vol. 129, p. 109923, Sep. 2020, doi: 10.1016/j.rser.2020.109923.

[20] S. Sumathi, G. Gayathri, A. Jancy Rani, S. Deepalakshmi, and K. Karthikeyan, "Design and Implementation of Solar Tracking System using LDR Sensor," *Int. J. Adv. Sci. Eng.*, vol. 06, no. 03, pp. 1456– 1461, Feb. 2020, doi: 10.29294/IJASE.6.3.2020.14561461.

[21] M. H. Majeed, N. T. Alwan, S. E. Shcheklein, and A. V. Matveev, "Electromechanical solar tracker system for a parabolic dish with CPU water heater," *Mater. Today Proc.*, vol. 42, pp. 2346–2352, 2021, doi: 10.1016/j.matpr.2020.12.326.

[22] M. Das and E. K. Akpinar, "Determination of thermal and drying performances of the solar air dryer with solar tracking system: Apple drying test," *Case Stud. Therm. Eng.*, vol. 21, p. 100731, Oct. 2020, doi: 10.1016/j.csite.2020.100731.

[23] M. Ghassoul, "A dual solar tracking system based on a light to frequency converter using a microcontroller," *Fuel Commun.*, vol. 6, p. 100007, Mar. 2021, doi: 10.1016/j.jfueco.2020.100007.

[24] C. Jamroen, P. Komkum, S. Kohsri, W. Himananto, S. Panupintu, and S. Unkat, "A low-cost dual-axis solar tracking system based on digital logic design: Design and implementation," *Sustain. Energy Technol. Assess.*, vol. 37, p. 100618, Feb. 2020, doi: 10.1016/j.seta.2019.100618.

[25] H. Zlatanov and G. Weinrebe, "CSP and PV Solar Tracker Optimization Tool," *Energy Procedia*, vol. 49, pp. 1603–1611, 2014, doi: 10.1016/j.egypro.2014.03.169.

[26] J. K. Tharamuttam and A. K. Ng, "Design and Development of an Automatic Solar Tracker," *Energy Procedia*, vol. 143, pp. 629–634, Dec. 2017, doi: 10.1016/j.egypro.2017.12.738.

[27] M. Mirdanies, "Astronomy Algorithm Simulation for Two Degrees of Freedom of Solar Tracking Mechanism Using Clanguage," *Energy Procedia*, vol. 68, pp. 60–67, Apr. 2015, doi: 10.1016/j.egypro.2015.03.233. [28] E. V. Canale, A. Stan, V. M. Zafiu, and A. C. Dinu, "Automatic solar tracking system," *Int. J. Mechatron. Appl. Mech.*, vol. 1, no. 6, pp. 246–249, 2019, doi: 10.17683/ijomam/issue6.24.

[29] R. F. Fuentes-Morales *et al.*, "Control algorithms applied to active solar tracking systems: A review," *Sol. Energy*, vol. 212, pp. 203–219, Dec. 2020, doi: 10.1016/j.solener.2020.10.071.

[30] A. Aldair, A. Obed, and A. Halihal, "Design and Implementation of Neuro-Fuzzy Controller Using FPGA for Sun Tracking System," Iraqi J. Electr. Electron. Eng., vol. 12, no. 2, pp. 123–136, 2016, doi: 10.37917/ijeee.12.2.2.

[31] D. F. Da Silva and D. Acosta-Avalos, "Light dependent resistance as a sensor in spectroscopy setups using pulsed light and compared with electret microphones," *Sensors*, vol. 6, no. 5, pp. 514–525, 2006, doi: 10.3390/s6050514.

[32] A. H. Jaaz, H. A. Hasan, K. Sopian, M. H. Bin Haji Ruslan, and S. H. Zaidi, "Design and development of compound parabolic concentrating for photovoltaic solar collector: Review," *Renew. Sustain. Energy Rev.*, vol. 76, pp. 1108–1121, Sep. 2017, doi: 10.1016/j.rser.2017.03.127.

[33] S. Ahmad, S. Shafie, and M. Z. A. Ab Kadir, "Power Feasibility of a Low Power Consumption Solar Tracker," *Procedia Environ. Sci.*, vol. 17, pp. 494–502, 2013, doi: 10.1016/j.proenv.2013.02.064.

[34] Simulink/Matlab," *Procedia Environmental Sciences*, vol. 17, pp. 537–546, 2013, doi: 10.1016/j.proenv.2013.02.069.

[35] L. Louis, "Working Principle of Arduino and Using it as a Tool for Study and Research," *Int. J. Control Autom. Commun. Syst.*, vol. 1, no. 2, pp. 21–29, 2016, doi: 10.5121/ijcacs.2016.1203.